Spontaneous epileptiform activity in a rat model of bilateral subcortical band heterotopia

Surajit Sahu, Emmanuelle Buhler, Jean-Christophe Vermoyal, Françoise Watrin, Alfonso Represa, Jean-Bernard Manent, Jean-christophe Vermoyal, Jean-bernard Manent

Received: 25 September 2018 | Revised: 20 November 2018 | Accepted: 7 December 2018

DOI: 10.1111/epi.14633

FULL-LENGTH ORIGINAL RESEARCH

Epilepsia®

Spontaneous epileptiform activity in a rat model of bilateral subcortical band heterotopia

Surajit Sahu | **Emmanuelle Buhler** | **Jean-Christophe Vermoyal** | **Françoise Watrin** | **Alfonso Represa** | **Jean-Bernard Manent**

Neurobiology Institute of the Mediterranean (INMED), Aix-Marseille University, French National Institute of Health and Medical Research (INSERM) UMR1249, Marseille, France

Correspondence
Jean-Bernard Manent, INMED INSERM UMR1249, Marseille, France.
Email: jean-bernard.manent@inserm.fr

Funding information
French National Agency for Research, Grant/Award Number: Young Researcher Grant/ANR-16-CE17-0013-01; European Community, Grant/Award Number: 7th Framework programs/Health-F2-602531-2013

Summary

Objective: Malformations of cortical development are common causes of intellectual disability and epilepsy, yet there is a crucial lack of relevant preclinical models associating seizures and cortical malformations. Here, we describe a novel rat model with bilateral subcortical band heterotopia (SBH) and examine whether this model develops spontaneous epileptic seizures.

Methods: To generate bilateral SBH in rats, we combined RNAi-mediated knockdown of *Dcx* and in utero electroporation with a tripolar electrode configuration enabling simultaneous transfection of the two brain hemispheres. To determine whether bilateral SBH leads to epileptiform activity, rats of various ages were implanted for telemetric electrocorticographic recordings and histopathological examination was carried out at the end of the recording sessions.

Results: By 2 months, rats with bilateral SBH showed nonconvulsive spontaneous seizures consisting of spike-and-wave discharges (SWDs) with dominant frequencies in the alpha and theta bands and secondarily in higher-frequency bands. SWDs occurred during both the dark and the light period, but were more frequent during quiet awake state than during sleep. Also, SWDs were more frequent and lasted longer at older ages. No sex differences were found. Although frequencies and durations of SWDs were found to be uncorrelated with the size of SBH, SWDs were initiated in some occasions from brain hemispheres comprising a larger SBH. Lastly, SWDs exhibited absence-like pharmacological properties, being temporarily alleviated by ethosuximide administration.

Significance: This novel model of bilateral SBH with spontaneous epilepsy may potentially provide valuable new insights into causality between cortical malformations and seizures, and help translational research aiming at designing novel treatment strategies for epilepsy.

KEYWORDS
animal model, epilepsy, gray matter heterotopia, malformation of cortical development

1 | INTRODUCTION

Malformations of cortical development (MCDs) are the most frequent causes of childhood epilepsies, carrying a lifelong perspective of disability and reduced quality of life. MCDs range from macroscopic and diffuse cortical malformations, such as subcortical band heterotopia, to more subtle malformations, which include focal cortical dysplasia.[1,2] The precise incidence of MCDs is not known; however, they have been diagnosed with increased frequency since brain imaging techniques have been used. From these studies, it is estimated that 25%-40% of intractable or medication-resistant childhood epilepsy is attributable to MCDs and that at least 75% of patients with MCDs will have epilepsy.[1] A large number of MCDs have been identified and are now categorized by using their putative embryologic origin, identified genetic cause, and brain imaging data as classification criteria.[2] However, the physiopathological mechanisms relating MCDs to epilepsy remain largely unknown, and valid animal models mimicking clinically relevant human disorders are crucially lacking.

Subcortical band heterotopia (SBH) is a prototypical example of MCD associating altered cortical layering, intellectual disability, and drug-resistant epilepsy. SBH occurs when neocortical neurons fail to migrate to the correct location and accumulate in the white matter, forming a heterotopic band of neurons below the normally migrated cortex.[3] This neuronal migration disorder is caused by mutations in the *DCX* gene,[4–7] and mutations of *DCX* were identified in 100% of familial SBH phenotypes and 85%-90% of sporadic cases.[8,9] SBH in humans is associated with intellectual disability (68%) and epilepsy (85%-96%), and with a high proportion of drug-resistant seizures (78%).[9,10] Also, epilepsy surgery in SBH patients has poor outcome due to the deep localization and large extent of SBH, their proximity to functionally crucial cortical areas, and difficulties in precisely identifying the epileptogenic zone.[11] Importantly, pathomechanisms underlying epileptogenesis and seizure generation remain largely elusive in human patients.

Experimental SBH can be modeled in rats by knockdown (KD) of *Dcx* in embryonic brains using in utero electroporation and RNA interference.[12–15] A series of reports from our laboratory indicated that these *Dcx*-KD rats display altered neocortical excitability, increased propensity for convulsant-induced seizures at juvenile ages, and spontaneous seizures in adulthood.[15–19] Although it provides extremely valuable insights into the cellular and network mechanisms underlying epileptogenicity in brains with SBH, this rat model has some limitations. Whereas most human patients present with bilateral SBH, *Dcx*-KD rats only harbor a single unilateral SBH due to methodological constraints when generating them. Also, spontaneous seizures were rarely seen before adulthood in rats,[17] whereas epilepsy usually starts during childhood and infancy in most patients with SBH.[9] Because more severe clinical phenotypes are found associated with larger and bilateral SBH,[9] we reasoned that a rat model with bilateral SBH would result in a more severe epilepsy phenotype or in an earlier age of seizure onset, yet better mimicking the human situation.

Key Points

- The in utero RNAi-mediated knockdown of *Dcx* using a tripolar electroporation method reproducibly induces bilateral SBH in rats
- Adult rats with bilateral SBH show nonconvulsive spontaneous seizures consisting of SWDs that become more frequent and last longer at older ages
- Frequencies and durations of SWDs are uncorrelated with the SBH size, although SWDs are initiated on some occasions from brain hemispheres comprising larger SBH
- SWDs in rats with bilateral SBH exhibit absencelike pharmacological properties

Here, we describe a novel rat model with bilateral SBH (referred to as bilateral *Dcx*-KD rats) that we generated by combining RNAi-mediated KD of *Dcx* and in utero electroporation with a tripolar electrode configuration enabling simultaneous transfection of the two brain hemispheres. We performed telemetric electrocorticographic recordings at various ages to characterize the epilepsy phenotype, and conducted histopathological examination after recordings to correlate with anatomical findings.

2 | MATERIALS AND METHODS

Animal experiments were performed in agreement with European directive 2010/63/UE and received approval (2015040809544569_v2 [APAFIS#436]) from the French Ministry for Research.

2.1 | Tripolar in utero electroporation

Tripolar in utero electroporation was performed as described[20,21] with modifications. Timed pregnant Wistar rats (Janvier Labs) received buprenorphine (Buprecare, 0.03 mg/kg) and were anesthetized with sevoflurane

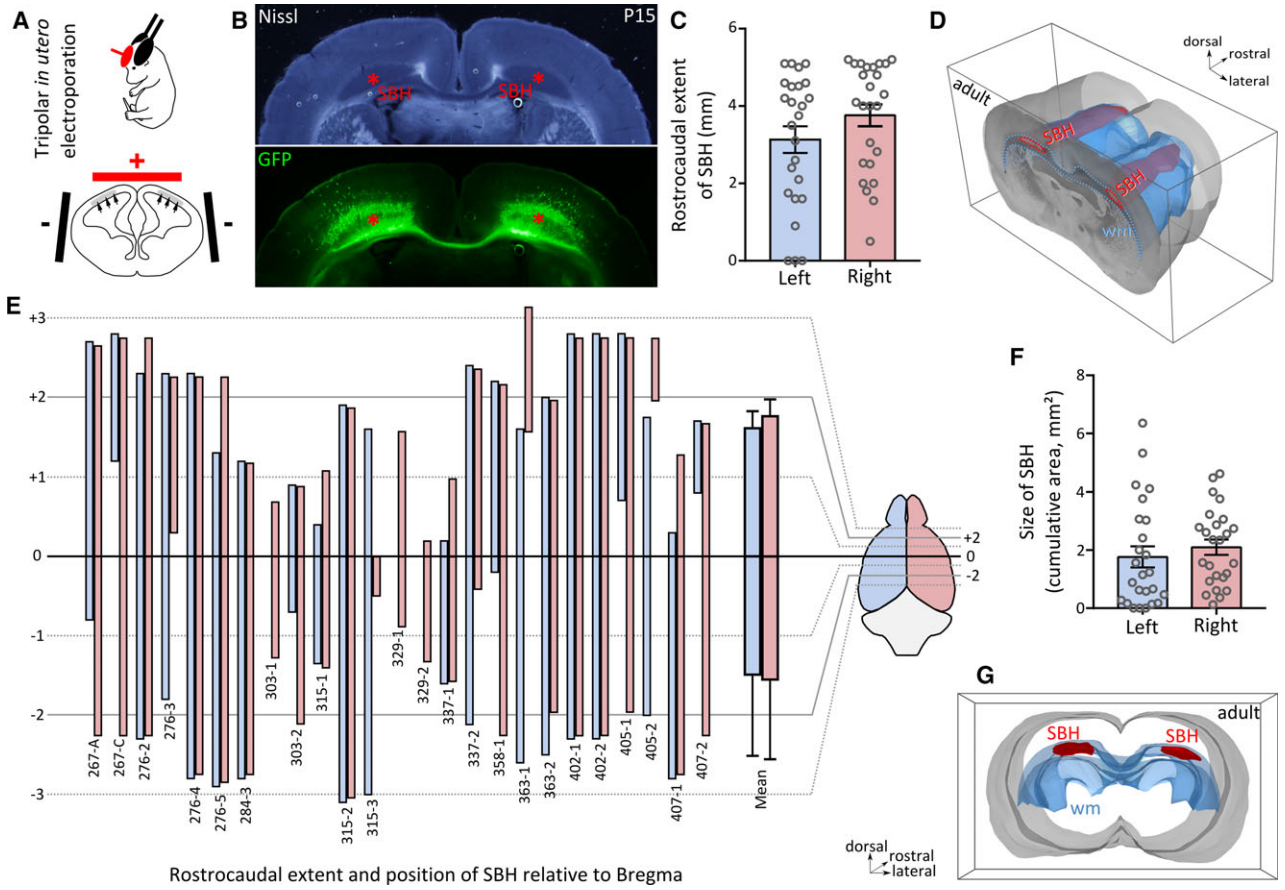

FIGURE 1 Anatomical features of bilateral *Dcx*-knockdown (KD) rats with bilateral subcortical band heterotopia. A, A schematic view of the tripolar in utero electroporation procedure, showing the placement of tweezer-type electrodes (black, negative pole) laterally pinching the embryo's head, and that of the third electrode (red, positive pole), placed rostrally and medially. The electric field induced by the potential applied to the electrodes enables a simultaneous and bilateral electroporation of cortical progenitors lining the lateral ventricles (gray area and arrows). B, Bright-field and fluorescent microphotographs of a postnatal day 15 (P15) neocortical section from a bilateral *Dcx*-KD rat showing bilateral subcortical band heterotopia (SBH; red asterisks), mostly composed of green fluorescent protein (GFP)-expressing neurons. Bundles of GFP-expressing callosal axons are also visible. C, Bar graphs showing the rostrocaudal extent of SBH in the left (blue) and right (pink) hemispheres of 25 adult bilateral *Dcx*-KD rats. D, Dorsolateral view of the rostral part of a three-dimensionally reconstructed adult brain with bilateral SBH (in red). The white matter (wm) is delineated in blue. E, Clustered bar graphs showing the rostrocaudal extent and position of SBH relative to bregma in the 25 *Dcx*-KD rats analyzed, in the left (blue) and right (pink) hemispheres. Animal identifier codes are given below each pairs of bars. F, Bar graphs showing the size of SBH (depicted as cumulative area) in the left (blue) and right (pink) hemispheres of 25 adult bilateral *Dcx*-KD rats. Open circles in C and F correspond to values for individual rats. G, Rear view of the same brain as in D

(4.5%) 30 minutes later. Uterine horns were exposed, and plasmid vectors (1 μg/μL) encoding shRNAs targeting the 3′ untranslated region of *Dcx* mRNA or encoding ineffective shRNAs with mutations creating mismatches[12] were microinjected bilaterally into the lateral ventricles of embryonic day 16 embryos, together with fast green dye and reporter constructs encoding green fluorescent protein or red fluorescent protein (0.5 μg/μL). After microinjections, electroporations were accomplished by delivering 50-V pulses (BTX ECM830 electroporator; Harvard Apparatus) across tweezer-type electrodes laterally pinching the head of each embryo through the uterus, and a third electrode (patent #WO/2012/153291) positioned at the brain midline (Figure 1A).

2.2 | Telemetric electroencephalographic recording

Under isoflurane anesthesia (induction 5%, maintenance 2%), rats were placed in a stereotaxic frame (David Kopf Instruments). Two or four holes were drilled through the skull above the somatosensory cortex (Figure 2A4) for electrode implantation using coordinates relative to the bregma (anteroposterior, −0.26; lateral, ±3.5). A reference electrode was placed on the cerebellum (anteroposterior, −12.3; lateral, ±3.0). Electrodes were secured with screws and mounted with dental acrylic. A subcutaneous pocket was created to insert the telemetry transmitter (CTA-F40 or EET-F40; DSI) on the left dorsal side of the rat.

Electroencephalographic (EEG) signals were digitized at 500 Hz and stored. Spike-and-wave discharges (SWDs) were identified offline by an automatic seizure detection module in NeuroScore (DSI), blind to the status of animals, which is usually revealed after histological analysis. Detection was performed using a dynamic threshold ratio of 1.5 (minimum value for detection is set to 100 μV) and corrected manually if needed. Spikes with duration ranging from 1 to 200 milliseconds were detected, and the minimum and maximum spike intervals within spike trains were 0.05 and 0.15 seconds, respectively. Only SWDs lasting >1 second were included in the analysis. Sleep-wake states were defined based on EEG amplitude, animal activity, and spectral power bands. Power spectral analyses were done using NeuroScore.

2.3 | Histology, tissue processing, and microscopy

At the end of EEG recordings, animals were deeply anesthetized with ketamine (Imalgene 1000, 100 mg/kg) and xylazine (Rompun 2%, 10 mg/kg) and perfused transcardially with 4% paraformaldehyde. Serial frontal sections (100 μm) were performed using a vibrating microtome (Leica Biosystems, Wetzlar, Germany), and images were taken using a stereomicroscope (SZX16; Olympus, Tokyo, Japan). Measurements were performed using Fiji[22] and tridimensional reconstructions using Free-D.[23]

2.4 | Statistical evaluation

Statistical analyses were performed using Prism 6 (GraphPad Software). Normality of the data distributions was tested using d'Agostino and Pearson test and Shapiro-Wilk normality test. All values are given as mean ± SEM. All tests were two-tailed, and significance level was set at $P < 0.05$.

3 | RESULTS

3.1 | Bilateral *Dcx*-KD rats present with bilateral SBH of variable positions and sizes

Experimental SBH can be modeled in rats by KD of *Dcx* in embryonic brains using unilateral in utero electroporation and RNA interference.[12,13,15] These rats, however, harbor a band heterotopia located in a single hemisphere, unlike most human patients harboring bilateral SBH.[9] To increase the relevance of experimental SBH regarding the human situation, we sought to develop a novel rat model with bilateral heterotopia. We utilized an in utero electroporation method and a triple electrode configuration (see Materials and Methods),[20,21] enabling simultaneous electroporation of the two brain hemispheres (Figure 1A) instead of a single hemisphere in the conventional settings.[14] We performed in utero RNAi-mediated KD of *Dcx* using this triple electrode configuration, and successfully induced the formation of SBH in the two hemispheres of juvenile (Figure 1B) and adult rats (Figure 1D). In most cases, SBH in bilateral *Dcx*-KD rats was located in the white matter below the dorsal portion of the neocortex (Figure 1B, 1D, and 1G). With the exception of its most rostral end located below the primary motor cortex, SBH were mainly located below the primary somatosensory cortex and barrel field. On average, SBH extended bilaterally over 3.13 ± 0.34 and 3.76 ± 0.28 mm in the rostrocaudal axis in the left and right hemisphere, respectively (N = 25 rats analyzed; Figure 1C–E). Their size, estimated from serial sections as cumulative areas, ranged from 1.76 ± 0.36 mm² in the left hemisphere to 2.10 ± 0.26 mm² in the right hemisphere (N = 25 rats analyzed; Figure 2F and 2G) with no left/right dominance on average. The average position of SBH in the rostrocaudal axis ranged from +1.6 ± 0.2 to −1.5 ± 0.3 mm relative to bregma in the left hemisphere (Figure 2E) and from 1.8 ± 0.2 to −1.6 ± 0.3 mm relative to bregma in the right hemisphere (N = 25 rats analyzed; Figure 2E). Although the overall extent and position of SBH appeared roughly homogeneous at the population level (see mean extent, Figure 2E), interindividual differences were clearly visible. Among the 25 rats we analyzed, a high proportion harbored bilateral SBH (88%, 22 rats), and only three rats had a band heterotopia in one hemisphere. Some animals were found with SBH extending symmetrically and bilaterally over similar rostrocaudal positions (8/25 rats, 32%), whereas others had a larger rostrocaudal extent in one of the two hemispheres. Of them, 13 rats (52%) had a larger extent in the right hemisphere and four rats (16%) had a larger extent in the left hemisphere (Figure 2E).

These observations indicate that *Dcx*-KD rats generated via tripolar in utero electroporation present with bilateral SBH resembling that seen in human patients, and constitute a novel preclinical model for subcortical band heterotopia.

3.2 | Rats with bilateral SBH exhibit spontaneous SWDs

To investigate whether the presence of bilateral SBH leads to epileptiform activity and to characterize it, we implanted subdural EEG electrodes in the somatosensory cortex of 25 bilateral *Dcx*-KD rats at variable ages (2-7 months), as well as in the somatosensory cortex of 17 control rats. The control group comprised several conditions: (1) three nonoperated wild-type rats ("wild-type" group); (2) two groups of four sham-operated rats, either only subjected to plasmid injection at embryonic ages ("injection only"

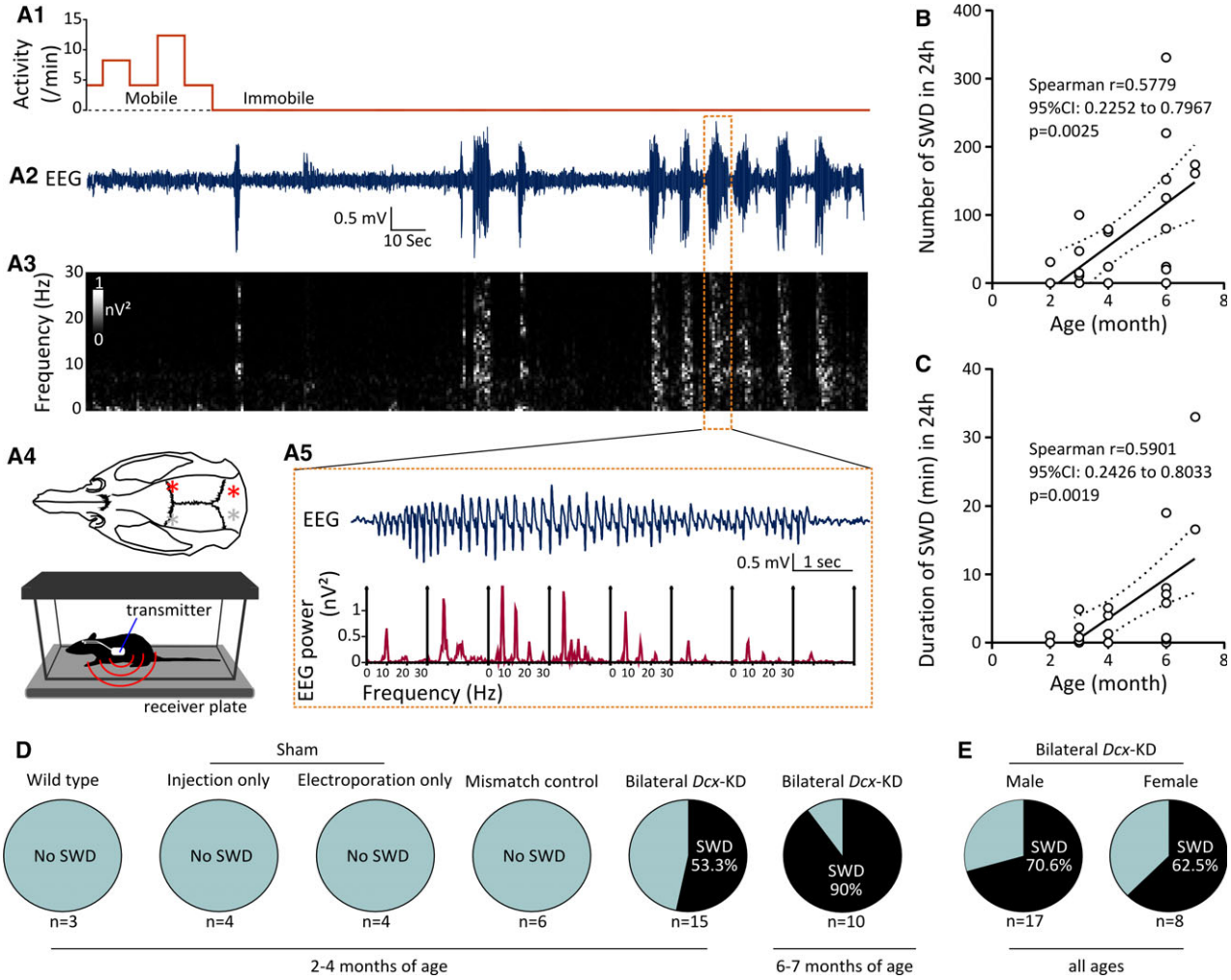

FIGURE 2 Characterization of epileptiform activity in bilateral *Dcx*-knockdown (KD) rats. A, Representative electroencephalographic (EEG) recording from the right primary somatosensory (S1) cortex of a bilateral *Dcx*-KD rat. A1, Animal movement, as detected by the activity sensor during EEG recording. A2, A3, EEG trace (A2), showing several epileptiform events, and the corresponding grayscale-coded time-frequency and spectral power analysis (A3). A5, EEG trace is further expanded to illustrate a selected epileptiform event (top) and the corresponding periodogram-based spectral density analysis of 1-second bins (bottom), with typical spike-and-wave discharge properties. A prominent ~9-Hz peak and harmonics are visible. A4, Top, Dorsal view of the rat skull showing locations (red and gray asterisks) of the two subdural recording electrodes over the S1 cortex, and reference electrodes placed over the cerebellum. Most rats were recorded unilaterally from the right hemisphere (red asterisks). A4, Bottom, Cartoon showing a freely behaving rat implanted with a telemetry unit, placed in a cage over the receiver plate. (B) Number of spike-and-wave discharges (SWDs) in 24 hours plotted as a function of age (in months), and best-fit linear regression line showing an age-dependent increase in the occurrence of SWDs in bilateral *Dcx*-KD rats. CI, confidence interval. (C) Duration of SWDs (in minutes) in 24 hours plotted as a function of age (in months), and best-fit linear regression line showing an age-dependent increase in the duration of SWDs in bilateral *Dcx*-KD rats. Dotted lines in B and C show 95% prediction bands of the regression lines. Open circles in B and C correspond to values for individual rats. (D) Pie charts showing the prevalence of SWDs in the control groups and bilateral *Dcx*-KD rats at variable ages. (E) Pie charts showing the prevalence of SWDs in male versus female bilateral *Dcx*-KD rats

group), or only subjected to electroporation at embryonic ages ("electroporation only" group); and (3) six mismatch rats injected and electroporated with mismatch plasmids not inducing SBH formation ("mismatch control" group). All rats were implanted with radiotelemetric transmitters allowing wireless, continuous sampling of EEG, body temperature, and locomotor activity in freely behaving, unrestrained conditions (Figure 2A4). At least 1 week postsurgery, continuous EEG recordings were performed over 3 consecutive days. EEG traces of sham-operated rats and mismatch controls were unremarkable, and not different from EEG traces of nonoperated wild-type rats (not illustrated). On the contrary, bilateral *Dcx*-KD rats were found to exhibit spontaneous electrographic seizures. These seizures were nonconvulsive, as no concurrent locomotor activity was detected by the activity sensor (Figure 2A1

and 2A2), as confirmed by video-monitoring or by direct observation by the experimenter in some animals. Besides locomotor arrest and immobility, repetitive facial grooming behavior or mild clonic facial movements were often noticed during seizures. Electrographic seizures in bilateral *Dcx*-KD rats consisted of trains of high-voltage, negative or/and positive spike-waves, resembling SWDs described in rodent models of absence epilepsy.[24–26] Time-frequency (Figure 2A3) and spectral power analysis (Figure 2A5) of SWDs revealed dominant frequencies in the alpha (8-13 Hz) and theta (4-8 Hz) bands, and secondarily in higher-frequency bands, consistently with what has been described in absence epilepsy models. On average, 98.18 ± 21.21 SWDs occurred over a 24-hour period (ie, 4.09 ± 0.88 SWDs/h), and individual SWDs lasted 3.54 ± 0.59 seconds (1669 SWDs from 17 rats were analyzed).

These observations indicate that bilateral SBH in this rat model leads to chronic spontaneous nonconvulsive seizures consisting of SWDs.

3.3 | Occurrence and duration of SWDs increase with age in rats with bilateral SBH

To detect potential age-dependent relationships with the occurrence or duration of SWDs in bilateral *Dcx*-KD rats, we computed a linear regression analysis. We detected a significant positive linear relationship between the age of animals and the number of SWDs they exhibited in 24 hours (Spearman $r = 0.5779$, 95% confidence interval [CI]: [0.2252, 0.7967], 25 pairs of variables analyzed, $P = 0.0025$; Figure 2B). We also found a significant positive linear relationship between the age of animals and the duration of the SWDs they exhibited in 24 hours (Spearman $r = 0.5901$, 95% CI: [0.2426, 0.8033], 25 pairs of variables analyzed, $P = 0.0019$; Figure 2C). When comparing the proportion of bilateral *Dcx*-KD rats exhibiting or not exhibiting SWDs at 2-4 months of age (53.3% with SWDs, 8/15 rats and 46.7% without SWDs, 7/15 rats) to that of *Dcx*-KD rats exhibiting or not exhibiting SWDs at 6-7 months of age (90% with SWDs, 9/10 rats and 10% without SWDs, 1/10 rats), we observed a 1.7-fold increase. A chi-square test was used to assess whether age and SWDs were associated in bilateral *Dcx*-KD rats, revealing a barely significant association (χ^2 [1 *df*] = 3.707, $P = 0.0542$; Figure 2D). Of note, none of the rats belonging to the different control groups exhibited SWDs at 2-4 months of age (Figure 2D).

Of the 25 bilateral *Dcx*-KD rats we analyzed, 17 were males and eight were females. Among the male group, 70.6% of rats exhibited SWDs (12/17) and 29.4% did not (5/17). Among the female group, 62.5% of rats exhibited SWDs (5/8) and 37.5% did not (3/8). A chi-square test was used to assess whether sex and SWDs were associated in bilateral *Dcx*-KD rats, revealing no statistically significant association (χ^2 [1 *df*] = 0.1635, $P = 0.6859$; Figure 2E).

These observations indicate that the prevalence, occurrence, and duration of SDWs increase with age in rats with bilateral SBH, with no influence of sex.

3.4 | Occurrence and duration of SWDs are unrelated to the extent of SBH

Because histopathological examinations after EEG recordings (see Figure 1) revealed that bilateral *Dcx*-KD rats presented with SBH of variable sizes, left-right positions, and rostrocaudal extents, we computed a linear regression analysis to detect potential anatomical relationships with the occurrence or duration of SWDs. We detected no significant linear relationship between the size of SBH and the number of SWDs they exhibited in 24 hours (Spearman $r = 0.02151$, 95% CI: [−0.3874, 0.4233], 25 pairs of variables analyzed, $P = 0.9187$; Figure 3A). We also found no significant linear relationship between the size of SBH and the duration of the SWDs they exhibited in 24 hours (Spearman $r = 0.01408$, 95% CI: [−0.3937, 0.4172], 25 pairs of variables analyzed, $P = 0.9467$; Figure 3B). Importantly, we detected no significant linear relationship between the size of SBH and the age of animals (Spearman $r = -01951$, 95% CI:[−0.548, 0.2168], 25 pairs of variables analyzed, $P = 0.3501$; not illustrated).

The majority of bilateral *Dcx*-KD rats we analyzed (20/25 rats) were implanted with a single EEG electrode, due to the technical limitations of the radiotelemetric transmitters we used, only enabling a single EEG channel. However, five bilateral *Dcx*-KD rats were implanted bilaterally with two EEG electrodes, allowing simultaneous sampling of EEG signals in the somatosensory cortices of the two brain hemispheres. We quantified the left-right predominance of SWD onsets in these rats, and observed variable situations. Two rats exhibited a clear right-side predominance of SWD onset with 100% of SWDs (rat 337-1, 20/20 SWDs) and 98.18% of SWDs (rat 402-2, 325/331 SWDs) detected first on the right EEG electrode (Figure 3C). One rat exhibited a clear left-side predominance of SWD onset with 63.63% (rat 405-1, 140/220 SWDs) of SWDs detected first on the left EEG electrode (Figure 3C). One rat exhibited SWDs mainly (57.5%) detected simultaneously by the two EEG electrodes (rat 337-2, 46/80 SWDs), other SWDs (35%) being detected first by the left EEG electrode (28/80 SWDs), and the remaining ones (7.5%) by the right EEG electrode (6/80 SWDs; Figure 3C and 3D). One rat exhibited SWDs equally detected (50%) either simultaneously by the two EEG electrodes (rat 402-1, 12/24 SWDs) or first by the right EEG electrode (12/24 SWDs; Figure 3C).

Among the three rats with a clear left or right predominance of SWD onset, only one rat had a larger SBH in the

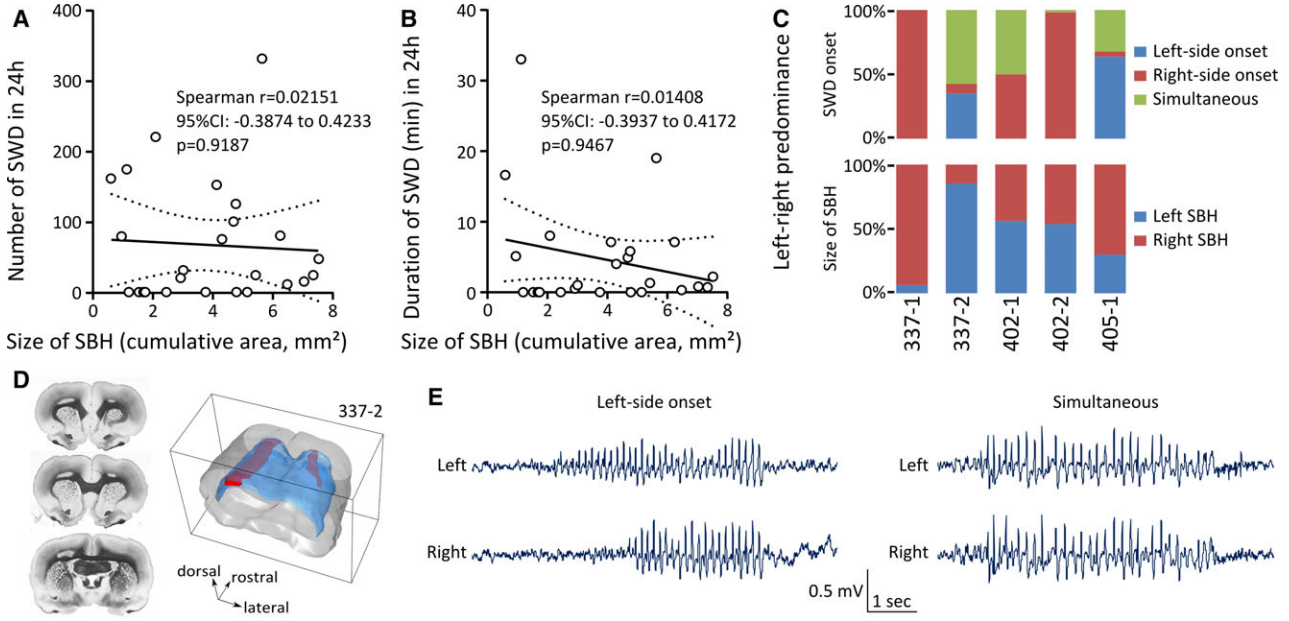

FIGURE 3 Spike-and-wave discharges (SWDs) in bilateral *Dcx*-knockdown (KD) rats are unrelated to the size of subcortical band heterotopia (SBH), although left-right dominance exists. A, Number of SWDs in 24 hours plotted as a function of the size of SBH (depicted as cumulative area), and best-fit linear regression line showing no relation between SBH size and the occurrence of SWDs. CI = confidence interval. B, Duration of SWDs (in minutes) in 24 hours plotted as a function of the size of SBH (depicted as cumulative area), and best-fit linear regression line showing no relation between SBH size and the duration of SWDs. Dotted lines in A and B show 95% prediction bands of the regression lines. Open circles in A and B correspond to values for individual rats. C, Top, Stacked bar graphs showing the proportion of SWDs with a left- or right-side onset, or with simultaneous onset in five bilateral *Dcx*-KD rats implanted bilaterally in primary somatosensory (S1) cortex of the two brain hemispheres. Bottom, Stacked bar graphs showing the size of SBH in the left versus right hemisphere (expressed as percentage of the total SBH size) in the same rats. D, Serial frontal sections and dorsolateral view of the three-dimensionally reconstructed brain of rat 337-2, illustrating a larger rostrocaudal extent of the left SBH as compared to the right SBH (left and right SBH are in red; white matter is in blue). E, Examples of electroencephalographic traces simultaneously sampled from the left and right S1 cortex of rat 337-2, showing SWDs with left-side onset (left panel) and that were simultaneously detected (right panel)

dominant hemisphere (rat 337-1; Figure 3C). The other two rats had either SBH of similar size in both hemispheres (rat 402-2) or a larger SBH in the hemisphere opposite to the dominant one (rat 405-1; Figure 3C). When omitting SWDs simultaneously detected by the two EEG electrodes, left-side onsets were predominant over right-side onsets in one rat with a larger SBH in the left hemisphere (35% vs 7.5%, rat 337-2). When omitting simultaneously detected SWDs, right-side onsets were predominant in two rats with SBH of similar size in both hemispheres (rats 402-1 and 402-2; Figure 3C).

The observations indicate that the occurrence and duration of SWDs are unrelated to the size of the malformation in rats with bilateral SBH. However, a left or right predominance of SWD onsets could be seen in some individuals.

3.5 | Occurrence of SWDs during the natural sleep/wake cycle in rats with bilateral SBH

To detect a preferential occurrence of SWDs during the dark/light period in bilateral *Dcx*-KD rats, we quantified the proportion of SWD events occurring in each period. Although SWDs were reported to occur preferentially during the dark rather than during the light period in absence epilepsy models,[24,25,27] we found that SWDs in bilateral *Dcx*-KD rats occurred equally during the dark and light periods (55.53% ± 3.12 during dark and 44.47% ± 3.12 during light, Wilcoxon matched-pairs signed rank test, $P = 0.1228$, n = 17; Figure 4A and 4B). We further characterized the occurrence of SWDs during the natural sleep-wake cycle and observed that, although SWDs can be seen during sleep, they preferentially occurred in the awake state (72.71% ± 7.532 during the awake state and 27.3% ± 7.529 during the sleep state, Wilcoxon matched-pairs signed rank test, $P = 0.0098$, n = 12; Figure 4C), and especially during quiet wake and immobility (see also Figure 2A1 and 2A2).

We went on to characterize EEG properties during the awake state, sleep states, and SWDs by performing power spectrum and power band analysis at different vigilant states and during SWDs (Figure 4D-F). As described above (Figure 2A3 and 2A5), the power spectrum of SWDs revealed a sharp and prominent 9-Hz peak, and additional sharp peaks in harmonic frequencies, although with lower

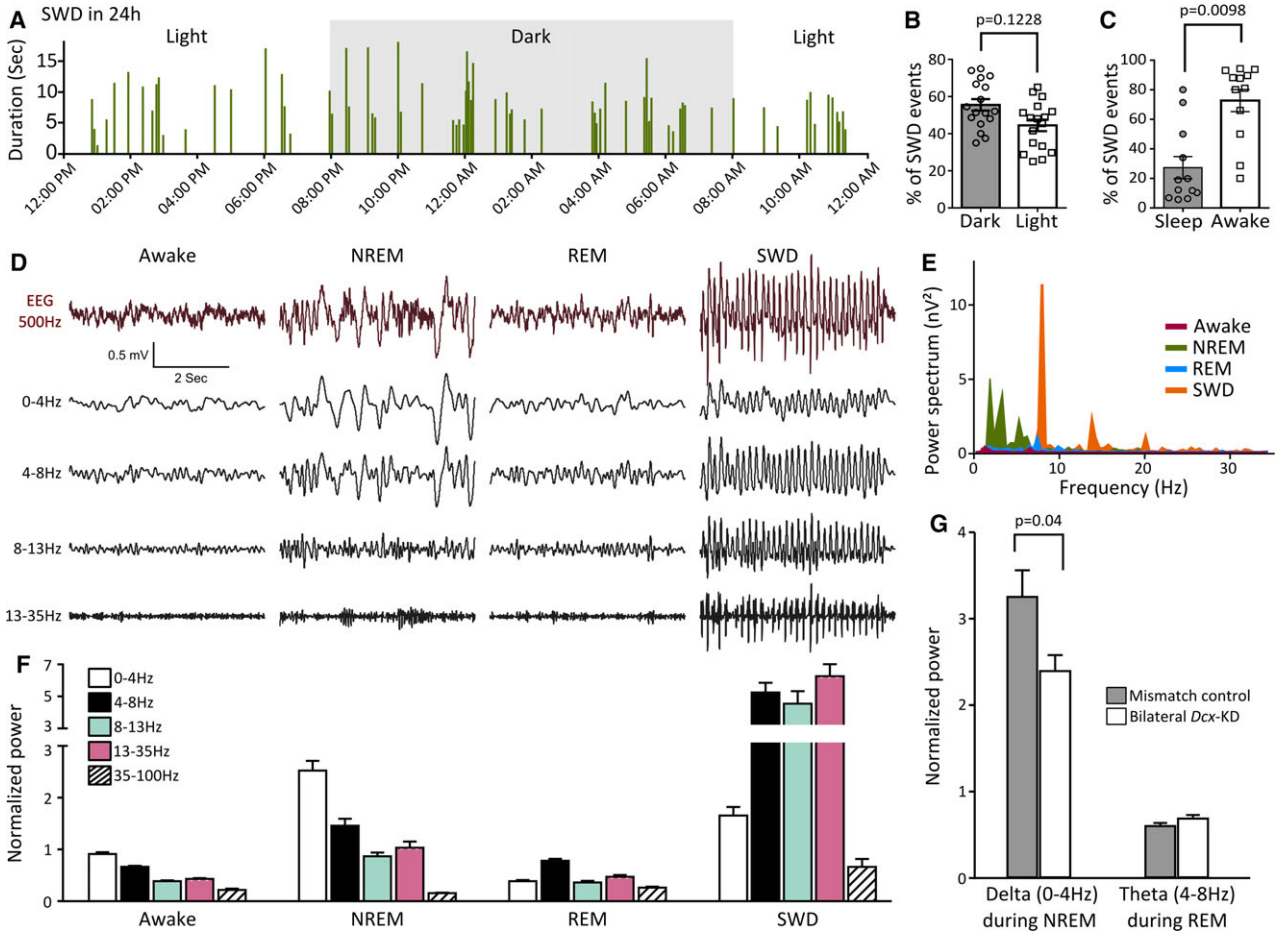

FIGURE 4 Spike-and-wave discharges (SWDs) across the natural sleep/wake cycle in bilateral *Dcx*-knockdown (KD) rats. A, Bar graph illustrating the occurrence and duration of SWDs across different phases of the dark-light cycle in a representative bilateral *Dcx*-KD rat. Individual bars indicate the occurrence of an SWD event, and their height show their duration (in seconds). B, C, Bar graphs showing the percentage of SWD events occurring during the dark and the light period (B), and during sleep and awake state (C). Open circles and squares in B and C correspond to values for individual rats. D, F, Representative raw and band-pass filtered electroencephalographic (EEG) traces at different vigilant states and during SWDs (D) and corresponding power band analysis (F). Averaged and normalized power values from 13 bilateral *Dcx*-KD rats were used. NREM, non–rapid eye movement; REM, rapid eye movement. E, Comparative power spectrum analysis of short EEG traces (2 seconds, 0-35 Hz) sampled during SWDs, wake, and NREM and REM sleep, showing a dominant ~9-Hz peak of high power during SWDs, accompanied by other peaks at harmonic frequencies. G, Bar graphs illustrating normalized delta during NREM and theta during REM in bilateral *Dcx*-KD rats compared to mismatch controls

power (Figure 4E), consistently with what was reported in other rodent models with SWDs.[28] In contrast, spectral power during rapid eye movement (REM) sleep or in the awake state was lower, with no prominent peak visible (Figure 4E). During non-REM sleep, however, several peaks in the alpha (0-4 Hz) and theta (4-8 Hz) range were identified, although with lesser power than the prominent 9-Hz peak seen during SWDs (Figure 4E). Power band analysis of averaged and normalized power values confirmed these observations (Figure 4F), and indicated a much higher power during SWDs than during any other vigilant states. We also examined the EEG power bands at different vigilant states in bilateral *Dcx*-KD rats compared to mismatch controls, and found a significantly decreased delta power during non-REM sleep ($P = 0.04$, 19 bilateral *Dcx*-KD rats and 11 mismatch rats analyzed; Figure 4G), suggestive of a decreased sleep quality in rats with bilateral SBH, as well as an unaltered theta power during REM sleep (Figure 4G).

Together, these observations indicate that SWDs in rats with bilateral SBH preferentially occur during the awake state, and especially during quiet wake and immobility.

3.6 | SWDs are modulated by ethosuximide in rats with bilateral SBH

SWDs in human patients and rodent models share unique pharmacological properties in that they are alleviated by

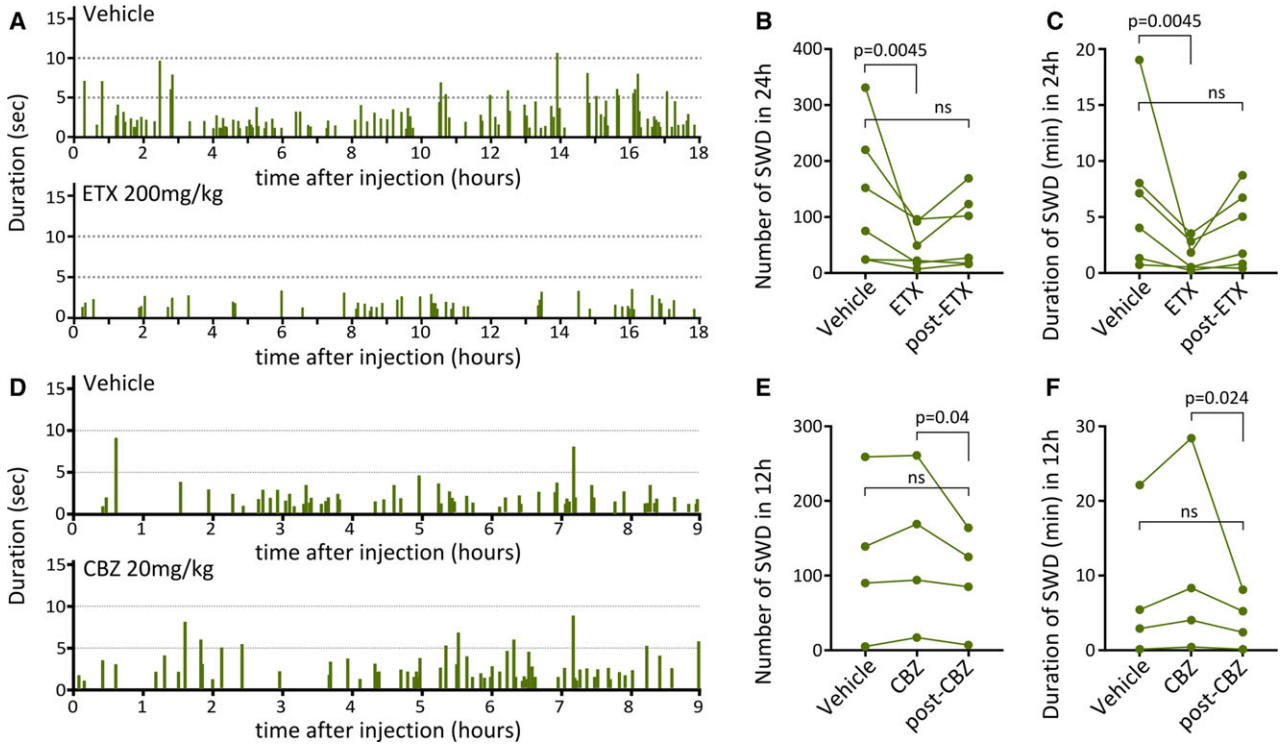

FIGURE 5 Spike-and-wave discharges (SWDs) in bilateral *Dcx*-knockdown (KD) rats are modulated by ethosuximide (ETX). A, Bar graphs illustrating the occurrence and duration (in seconds) of SWDs for 18 hours after vehicle (top) and ETX (bottom) administration to a representative bilateral *Dcx*-KD rat. SWD events (individual bars) are less frequent and of shorter duration (lower height of individual bars) after ETX. B, C, Line graphs showing the number of SWD events (B), and their duration (in minutes) in 24 hours (C) after vehicle and ETX administration, and after a 2-day recovery period after ETX administration (post-ETX). ns, not significant. D, Bar graphs illustrating the occurrence and duration (in seconds) of SWDs for 9 hours after vehicle (top) and carbamazepine (CBZ; bottom) administration to a representative bilateral *Dcx*-KD rat. E, F, Line graphs showing the number of SWD events (E), and their duration (in minutes) in 12 hours (F) after vehicle and CBZ administration, and after a 2-day recovery. Green dots in B, C, E, F correspond to values for individual rats

ethosuximide administration and are exacerbated by carbamazepine (CBZ) treatment.[29,30] To further understand the properties of SWDs in bilateral *Dcx*-KD rats, we administered ethosuximide (ETX; 200 mg/kg intraperitoneal) to six bilateral *Dcx*-KD rats and quantified using EEG recordings the occurrence and duration of SWDs for 24 hours after vehicle or ETX treatment, as well as 2 days later. We found a drastic reduction in both the number and duration of SWDs occurring over a 24-hour period after ETX administration (Friedman test, $P = 0.0017$, Dunn multiple comparisons test, $P = 0.0045$ for vehicle vs ETX; Figure 5A-C), which returned to baseline values 2 days later (Dunn multiple comparisons test, $P = 0.1299$ for vehicle vs post-ETX; Figure 5A-C).

We also administered CBZ (20 mg/kg intraperitoneal) to four bilateral *Dcx*-KD rats and quantified the occurrence and duration of SWDs for 12 hours after vehicle or CBZ treatment, as well as 2 days later. Contrary to ETX treatment, CBZ induced a nonsignificant increase in the number and duration of SWDs (Friedman test, $P = 0.0017$, Dunn multiple comparisons test, $P = 0.2313$ and $P = 0.3348$ for vehicle vs CBZ, number and duration of SWDs, respectively; Figure 5E-G), which returned to baseline values 2 days later (Dunn multiple comparisons test, $P = 0.9999$ and $P = 0.8665$ for vehicle vs post CBZ, number and duration of SWDs, respectively; Figure 5E-G).

Because ETX is the first-choice anticonvulsant for absence seizures, these observations further validate the SWD nature of the spontaneous seizures seen in rats with bilateral SBH.

4 | DISCUSSION

Here, we report that the in utero RNAi-mediated KD of *Dcx* by means of a tripolar electroporation method reproducibly induces bilateral SBH associated with a chronic epileptic condition characterized by SWDs in rats. This novel model of bilateral SBH with spontaneous epilepsy may potentially provide valuable new insight into causality between SBH and seizures, which is still largely elusive in human patients.

SBH patients typically present with epilepsy (85%-96% depending on patient cohorts) and have their first seizure in the first decade.[9,31] Seizure types are highly variable from patient to patient, and vary from focal onset seizures (partial seizures) to generalized onset seizures. Simple/complex partial seizures are most often described (68%-69%); drop attacks (26%-30%), absence seizures (23%-29%), and myoclonic seizures (14%-16%) are frequently found alone or in combination (43%-60%) as well as generalized tonic-clonic seizures (19%-57%).[9,31] Patients with West syndrome and Lennox-Gastaut syndrome have also been described.[9,31–35] Importantly, a high proportion of drug resistance (65%-78%) is reported,[9,31] and surgical treatment yields poor outcomes.[11,36,37] Seizure types found at epilepsy onset often evolve, and a combination of multiple seizure types could be observed as epilepsy progresses.[9,31] Given the diversity of seizure types described, no clear disease-specific EEG pattern is associated with SBH, and various abnormal patterns are described.

In *Dcx*-KD rats with bilateral SBH described herein, a single seizure pattern consisting of SWDs was observed, and its electrographic and pharmacological properties were similar to those seen in human patients[29,30] and rodent models[24,25,27,38] of absence seizures. In *Dcx*-KD rats with unilateral SBH, we previously reported a similar electrographic pattern of SWDs,[17] although its pharmacological profile was not investigated. The *tish* rat, another rat model with bilateral subcortical heterotopia, which appeared spontaneously in a colony of Sprague Dawley rats and has spontaneous partial seizures,[39] was recently reinvestigated.[40] These investigations indicated that electrographic abnormalities in *tish* rats also consisted of SWDs. In all, these observations in different rat models suggest that a chronic epileptic condition characterized by SWDs could be induced by the presence of unilateral or bilateral SBH. Given that about a quarter of SBH patients present with absence epilepsy (see above), this suggests a possible causal link between SBH and absence seizures in these patients, although the underlying pathomechanisms remain unresolved.

Surface EEG in SBH patients with absence seizures typically shows generalized bilateral SWDs predominantly in frontal regions.[33,35] Given the anterior-biased location of SBH in most female patients with *DCX* mutations[41,42] and the particular involvement of frontal regions in absence epilepsy,[43–45] it is tempting to speculate that seizures are primarily generated by epileptogenic networks located in frontal regions in SBH patients with absence epilepsy. Although stereo-EEG recordings have been conducted in a few SBH patients,[46–48] none has been performed in absence patients with SBH that could corroborate this idea, to our knowledge. In bilateral *Dcx*-KD rats implanted bilaterally with two EEG electrodes, SWDs were always recorded from both hemispheres, although with shorter latencies in one or the other, suggesting possible asymmetric onsets depending on the location and extent of SBH, or depending on those of epileptogenic networks.

Disregarding the seizure type, it is still unclear which of the two structures—the SBH or the overlying cortex—is responsible for seizure generation, and EEG–functional magnetic resonance imaging studies have revealed blood oxygenation level–dependent changes extending to both structures during seizure events.[49,50] These observations suggest that extended or multiple focal seizure generators could exist, in agreement with the multifocal nature of epileptic activity in SBH patients, the poor surgical outcome of focal resection of epileptogenic tissue,[11] and relatively greater outcomes of anterior corpus callosotomy.[11,36,37] The situation is even more complex because a high proportion of patients (64%) present with multiple seizure types in combination,[31] likely initiated from distinct seizure generators. In bilateral *Dcx*-KD rats, a single seizure type was found, which may facilitate future investigations of the physiopathological mechanisms relating SBH to epilepsy.

More severe clinical phenotypes were found associated with larger SBH in large cohorts of patients with *DCX* mutations.[9] This clinical observation prompted us to generate this novel model with larger and bilateral SBH, reasoning that the epilepsy phenotype may be distinct, more severe or with an earlier age of onset, as compared with the previous model with unilateral SBH.[17] Although the electrographic pattern of seizures was not different in the two models, epilepsy onset in bilateral *Dcx*-KD rats was found to be shifted toward earlier ages (2 vs 6 months), in keeping with this idea. However, we revealed no association between the size of bilateral SBH and the frequencies or durations of SWDs, although SWDs were initiated on some occasions from brain hemispheres comprising larger SBH.

In all, we characterized herein a novel rat model with bilateral SBH and chronic spontaneous nonconvulsive seizures, generated by manipulating the expression of *Dcx*, one of the main causative genes of SBH in humans. This model, associating genetic, histopathological, and electroclinical features relevant to those seen in human patients, may potentially provide valuable new insights into causality between SBH and seizures. Similar to other experimental model systems, our rat model has limitations that may preclude the generalization of conclusions derived from its study. Although a great diversity of seizure types is described in SBH patients, bilateral *Dcx*-KD rats present with a single seizure type, and thus only reproduce the symptomatology of a subpopulation of patients. Given the clinical-radiological heterogeneity of *DCX*-related disorders, with severe sporadic and milder familial form of SBH,

each associated with various *DCX* mutations,[9] and the absence of a clear disease-specific EEG pattern, it is not unexpected that a single experimental model cannot reflect such diversity. Despite these limitations, future work aiming at identifying and characterizing epileptogenic networks in bilateral *Dcx*-KD rats may be helpful for clarifying the relative contribution of the SBH and the overlying cortex to epilepsy. Of interest, we have recently identified circuit-level abnormalities in the overlying cortex of bilateral *Dcx*-KD rats prior to epilepsy onset,[51] suggesting that this model may also be useful for investigating mechanisms related to the development of epilepsy. Lastly, further investigations and behavioral tests are required to assess whether concurrent epilepsy comorbidities are present in bilateral *Dcx*-KD rats.

ACKNOWLEDGMENT

This study was supported by the French National Agency for Research (SILENCing excitability of epileptogenic networks in Early Epileptic Disorders [SILENCEED], Young Researcher Grant, ANR-16-CE17-0013-01 to J.-B.M.) and European Community 7th Framework programs (Development and Epilepsy—Strategies for Innovative Research to improve diagnosis, prevention and treatment in children with difficult to treat Epilepsy [DESIRE], Health-F2-602531-2013 to A.R.). E.B., F.W., and J.-B.M. are funded by INSERM (French National Institute of Health and Medical Research). A.R. is funded by CNRS (French National Center for Scientific Research). J.-C.V. is funded by the French Ministry for Higher Education and Research, and Aix-Marseille University. We thank Dr L. Cancedda for providing the patented third electrode used for tripolar electroporation; Dr L. Petit for his technical support with electronics; Dr M. Jalabert and Y. Chauvin for technical assistance at the early stage of the study; and Drs M. Milh, P. P. Lenck-Santini, and M. Minlebaev for insightful comments and critical reading of the manuscript.

DISCLOSURE

The authors have no conflicts of interest to report. We confirm that we have read the Journal's position on issues involved in ethical publication and affirm that this report is consistent with those guidelines.

ORCID

Surajit Sahu https://orcid.org/0000-0002-9529-3939
Françoise Watrin https://orcid.org/0000-0003-2087-412X
Alfonso Represa https://orcid.org/0000-0002-5096-8939
Jean-Bernard Manent https://orcid.org/0000-0002-2436-8593

REFERENCES

1. Guerrini R, Dobyns WB. Malformations of cortical development: clinical features and genetic causes. Lancet Neurol. 2014;13:710–26.
2. Desikan RS, Barkovich AJ. Malformations of cortical development. Ann Neurol. 2016;80:797–810.
3. Barkovich AJ, Jackson DEJ, Boyer RS. Band heterotopias: a newly recognized neuronal migration anomaly. Radiology. 1989;171:455–8.
4. Pinard JM, Motte J, Chiron C, et al. Subcortical laminar heterotopia and lissencephaly in two families: a single X linked dominant gene. J Neurol Neurosurg Psychiatry. 1994;57:914–20.
5. des Portes V, Francis F, Pinard JM, et al. Doublecortin is the major gene causing X-linked subcortical laminar heterotopia (SCLH). Hum Mol Genet. 1998;7:1063–70.
6. Gleeson JG, Allen KM, Fox JW, et al. Doublecortin, a brain-specific gene mutated in human X-linked lissencephaly and double cortex syndrome, encodes a putative signaling protein. Cell. 1998;92:63–72.
7. Pilz DT, Matsumoto N, Minnerath S, et al. LIS1 and XLIS (DCX) mutations cause most classical lissencephaly, but different patterns of malformation. Hum Mol Genet. 1998;7:2029–37.
8. Matsumoto N, Leventer RJ, Kuc JA, et al. Mutation analysis of the DCX gene and genotype/phenotype correlation in subcortical band heterotopia. Eur J Hum Genet. 2001;9:5–12.
9. Bahi-Buisson N, Souville I, Fourniol FJ, et al. New insights into genotype-phenotype correlations for the doublecortin-related lissencephaly spectrum. Brain. 2013;136:223–44.
10. Dobyns WB. The clinical patterns and molecular genetics of lissencephaly and subcortical band heterotopia. Epilepsia. 2010;51 (Suppl 1):5–9.
11. Bernasconi A, Martinez V, Rosa-Neto P, et al. Surgical resection for intractable epilepsy in "double cortex" syndrome yields inadequate results. Epilepsia. 2001;42:1124–9.
12. Bai J, Ramos RL, Ackman JB, et al. RNAi reveals doublecortin is required for radial migration in rat neocortex. Nat Neurosci. 2003;6:1277–83.
13. Ramos RL, Bai J, LoTurco JJ. Heterotopia formation in rat but not mouse neocortex after RNA interference knockdown of DCX. Cereb Cortex. 2006;16:1323–31.
14. LoTurco J, Manent J, Sidiqi F. New and improved tools for in utero electroporation studies of developing cerebral cortex. Cereb Cortex. 2009;19(Suppl 1):i120–5.
15. Manent J, Wang Y, Chang Y, et al. Dcx reexpression reduces subcortical band heterotopia and seizure threshold in an animal model of neuronal migration disorder. Nat Med. 2009;15:84–90.
16. Ackman JB, Aniksztejn L, Crepel V, et al. Abnormal network activity in a targeted genetic model of human double cortex. J Neurosci. 2009;29:313–27.
17. Lapray D, Popova IY, Kindler J, et al. Spontaneous epileptic manifestations in a DCX knockdown model of human double cortex. Cereb Cortex. 2010;20:2694–701.

18. Petit LF, Jalabert M, Buhler E, et al. Normotopic cortex is the major contributor to epilepsy in experimental double cortex. Ann Neurol. 2014;76:428–42.
19. Martineau FS, Sahu S, Plantier V, et al. Correct laminar positioning in the neocortex influences proper dendritic and synaptic development. Cereb Cortex. 2018;28:2976–90.
20. dal Maschio M, Ghezzi D, Bony G, et al. High-performance and site-directed in utero electroporation by a triple-electrode probe. Nat Commun. 2012;3:960.
21. Szczurkowska J, Cwetsch AW, dal Maschio M, et al. Targeted in vivo genetic manipulation of the mouse or rat brain by in utero electroporation with a triple-electrode probe. Nat Protoc. 2016;11:399–412.
22. Schindelin J, Arganda-Carreras I, Frise E, et al. Fiji: an open-source platform for biological-image analysis. Nat Methods. 2012;9:676–82.
23. Andrey P, Maurin Y. Free-D: an integrated environment for three-dimensional reconstruction from serial sections. J Neurosci Methods. 2005;145:233–44.
24. Robinson PF, Gilmore SA. Spontaneous generalized spike-wave discharges in the electrocorticograms of albino rats. Brain Res. 1980;201:452–8.
25. Vergnes M, Marescaux C, Micheletti G, et al. Spontaneous paroxysmal electroclinical patterns in rat: a model of generalized non-convulsive epilepsy. Neurosci Lett. 1982;33:97–101.
26. Coenen AM, Van Luijtelaar EL. The WAG/Rij rat model for absence epilepsy: age and sex factors. Epilepsy Res. 1987;1:297–301.
27. Van Luijtelaar EL, Coenen AM. Circadian rhythmicity in absence epilepsy in rats. Epilepsy Res. 1988;2:331–6.
28. Sitnikova E, Hramov AE, Koronovsky AA, et al. Sleep spindles and spike-wave discharges in EEG: their generic features, similarities and distinctions disclosed with Fourier transform and continuous wavelet analysis. J Neurosci Methods. 2009;180:304–16.
29. Browne TR, Dreifuss FE, Dyken PR, et al. Ethosuximide in the treatment of absence (petit mal) seizures. Neurology. 1975;25:515–24.
30. Snead OC, Hosey LC. Exacerbation of seizures in children by carbamazepine. N Engl J Med. 1985;313:916–21.
31. D'Agostino MD, Bernasconi A, Das S, et al. Subcortical band heterotopia (SBH) in males: clinical, imaging and genetic findings in comparison with females. Brain. 2002;125:2507–22.
32. Palmini A, Andermann F, Aicardi J, et al. Diffuse cortical dysplasia, or the "double cortex" syndrome: the clinical and epileptic spectrum in 10 patients. Neurology. 1991;41:1656–62.
33. Bauer J, Elger CE. Band heterotopia: a rare cause of generalized epileptic seizures. Seizure. 1994;3:153–5.
34. Granata T, Battaglia G, D'Incerti L, et al. Double cortex syndrome: electroclinical study of three cases. Ital J Neurol Sci. 1994;15:15–23.
35. Ricci S, Cusmai R, Fariello G, et al. Double cortex. A neuronal migration anomaly as a possible cause of Lennox-Gastaut syndrome. Arch Neurol. 1992;49:61–4.
36. Landy HJ, Curless RG, Ramsay RE, et al. Corpus callosotomy for seizures associated with band heterotopia. Epilepsia. 1993;34:79–83.
37. Vossler DG, Lee JK, Ko TS. Treatment of seizures in subcortical laminar heterotopia with corpus callosotomy and lamotrigine. J Child Neurol. 1999;14:282–8.
38. Van Luijtelaar E, Depaulis A. Genetic models of absence epilepsy in the rat. In: Pitkänen A, Schwartzkroin P, Moshé S, eds. *Models of seizures and epilepsy*. 1st ed. San Diego, CA: Elsevier; 2006:233–48.
39. Lee KS, Schottler F, Collins JL, et al. A genetic animal model of human neocortical heterotopia associated with seizures. J Neurosci. 1997;17:6236–42.
40. Grosenbaugh D, Joshi S, Lee K, et al. A spontaneous deletion in Eml1 underlies the bilateral cortical malformation in the tish rat model of subcortical heterotopia. Program No. 293.03. 2017 Neuroscience Meeting Planner. Washington, DC: Society for Neuroscience; 2017. Available at: http://www.abstractsonline.com/pp8/#!/4376/presentation/10188. Accessed August 2, 2018.
41. Gleeson JG, Luo RF, Grant PE, et al. Genetic and neuroradiological heterogeneity of double cortex syndrome. Ann Neurol. 2000;47:265–9.
42. Leventer RJ. Genotype-phenotype correlation in lissencephaly and subcortical band heterotopia: the key questions answered. J Child Neurol. 2005;20:307–12.
43. Holmes MD, Brown M, Tucker DM. Are "generalized" seizures truly generalized? Evidence of localized mesial frontal and frontopolar discharges in absence. Epilepsia. 2004;45:1568–79.
44. Moeller F, LeVan P, Muhle H, et al. Absence seizures: individual patterns revealed by EEG-fMRI. Epilepsia. 2010;51:2000–10.
45. Carney PW, Masterton RAJ, Flanagan D, et al. The frontal lobe in absence epilepsy: EEG-fMRI findings. Neurology. 2012;78:1157–65.
46. Morrell F, Whisler W, Hoeppner T, et al. Electrophysiology of heterotopic gray matter in the "Double cortex" syndrome. Epilepsia. 1992;33(Suppl 3):l-140.
47. Lo Russo G, Tassi L, Cossu M, et al. Focal cortical resection in malformations of cortical development. Epileptic Disord. 2003;5(Suppl 2):S115–23.
48. Mai R, Tassi L, Cossu M, et al. A neuropathological, stereo-EEG, and MRI study of subcortical band heterotopia. Neurology. 2003;60:1834–8.
49. Kobayashi E, Bagshaw AP, Grova C, et al. Grey matter heterotopia: what EEG-fMRI can tell us about epileptogenicity of neuronal migration disorders. Brain. 2006;129:366–74.
50. Tyvaert L, Hawco C, Kobayashi E, et al. Different structures involved during ictal and interictal epileptic activity in malformations of cortical development: an EEG-fMRI study. Brain. 2008;131:2042–60.
51. Plantier V, Watrin F, Buhler E, et al. Direct and collateral alterations of functional cortical circuits in a rat model of subcortical band heterotopia. Cereb Cortex. 2018 Dec 7. [Epub ahead of print].

How to cite this article: Sahu S, Buhler E, Vermoyal J-C, Watrin F, Represa A, Manent J-B. Spontaneous epileptiform activity in a rat model of bilateral subcortical band heterotopia. *Epilepsia*. 2018;00:1–12. https://doi.org/10.1111/epi.14633